HHS Public Access

Author manuscript

J Am Acad Dermatol. Author manuscript; available in PMC 2018 February 01.

Published in final edited form as:

J Am Acad Dermatol. 2017 February ; 76(2): 209–216.e9. doi:10.1016/j.jaad.2016.09.008.

Rapid visualization of non-melanoma skin cancer

Ethan Walker, MD, PhD[1], **Margaret Mann, MD**[2], **Kord Honda, MD**[2], **Allison Vidimos, MD**[3], **Mark Schluchter, PhD**[4], **Brian Straight, PhD**[5], **Matthew Bogyo, PhD**[6,7], **Daniel Popkin, MD, PhD**[2], and **James P. Basilion, PhD**[1,8]

[1]Department of Biomedical Engineering, Case Western Reserve University, Cleveland, OH, USA

[2]Department of Dermatology, University Hospital, Cleveland, OH, USA

[3]Department of Dermatology, Cleveland Clinic Foundation, Cleveland, OH, USA

[4]Department of Epidemiology & Biostatistics, Case Western Reserve University, Cleveland, OH

[5]Akrotome Imaging Inc., Cleveland, OH 44106

[6]Department of Pathology, Stanford University, Stanford, CA, USA

[7]Department of Microbiology and Immunology, Stanford University, Stanford, CA, USA

[8]Department of Radiology and NFCR Center for Molecular Imaging, Case Western Reserve University, Cleveland, OH, USA

Abstract

Background—Mohs micrographic surgery (MMS) examines all margins of the resected sample and has a 99% cure rate. However, many non-melanoma skin cancers (NMSCs) are not readily amenable for MMS. This defines an unmet clinical need to assess the completeness of non-MMS resections during surgery to prevent re-excision/recurrence.

Objective—Examine the utility of quenched activity-based probe (QABP) imaging to discriminate cancerous versus normal skin tissue.

Methods—The QABP GB119 was applied to NMSC excised from 68 patients. We validated activation of the probe for H&E confirmed cancerous tissue versus normal skin tissue.

Results—Topical application of the probe differentiated basal cell carcinoma (BCC) and squamous cell carcinoma (SCC) from normal skin with overall estimated sensitivity and

Corresponding Author: James P. Basilion, Ph.D. Professor Departments of Radiology, Biomedical Engineering, and Pathology Case Center for Imaging Research, Case Western Reserve University, Wearn Building, Room B42, 11100 Euclid Ave. Cleveland Ohio, 44106-5056. james.basilion@case.edu; Tel: 216-983-3264; Fax: 216-844-4987.

Conflict of Interest Disclosures: Drs. Basilion and Bogyo are both board members and co-founders of Akrotome Imaging Inc. Dr. Straight is the CEO of Akrotome Imaging Inc. No other disclosures were reported.

Previous presentation: The abstract of this study was presented as an oral presentation at the World Molecular Imaging Congress; September 2–5, 2015; Honolulu, Hawaii.

IRB Status: These studies were approved by Case Western Reserve University Hospital IRB.

specificity [95% CI] of 0.989 [0.940–1.00] and 0.894 [0.769–0.965], respectively. Probe activation accurately defined peripheral margins of NMSC as compared to conventional H&E based pathology.

Limitations—This study only examined NMSC debulking excision specimens. The sensitivity and specificity for this approach using final NMSC excision margins will be clinically important.

Conclusions—These findings merit further studies to determine whether QABP technology may enable cost-effective increased cure rates for NMSC patients by reducing re-excision and recurrence rates with a rapid and easily interpretable technological advance.

Keywords

molecular optical imaging; quenched activity based probe; topical application; cathepsin-L; non-melanoma skin cancer; re-excision rate; cathepsin-B

Introduction

Non-melanoma skin cancers (NMSC) are the most common form of human cancer with approximately 3.5-million diagnosed in the USA in 2006 and approximately 4 million diagnosed each year hence[1,2]. Approximately 80% of all NMSC are basal cell carcinomas (BCC) with most of the remaining being squamous cell carcinomas (SCC).[3] Several approaches to ensure complete removal of diseased tissues with minimal resection of normal tissue have been developed, including Mohs micrographic surgery (MMS)[4,5] that checks margins during surgery and has the highest cure rate of all approaches (99%). However, conventional or non-MMS resection is the most common surgical approach for skin cancers representing approximately 75% of surgical procedures for BCC and SCC[1] and has much lower cure rates than MMS. Well-differentiated SCC cure rates approach 81% using non-MMS procedures but drops to 46% for poorly differentiated lesions[6]. Resections of BCC fare slightly better with approximately 93% cure rates[7]. Since rates are related to the size of margins that the dermatologist removes, conventional resections generally results in larger resections of normal tissue to ensure clear margins, which are determined by conventional pathology several days after the surgery[8,9]. Here we describe an easily interpretable methodology that could be cost-effectively deployed and rapidly executed to enable surgeons to better assess peripheral surgical margins, thus reducing the amount of normal tissue resected during conventional NMSC excisions.

The study presented exploits molecular imaging technology[10,11] to target overexpressed skin cancer-associated cathepsin proteases[12–16]. The technique uses a cysteine cathepsin selective class of quenched near-infrared fluorescent activity-based probes (QABPs)[17] effective for imaging tumor-expressed cathepsins, *in vitro* and *in vivo*[18–22], which are hydrophobic and readily penetrate the skin. Interaction of QABPs with target proteases results in de-quenching and production of a fluorescent signal. Here GB119 is employed to target cancer cysteine cathepsin enzymes to discriminate NMSC from normal skin *ex vivo* creating a 2D-fluorescent map for each sample. Specifically, *ex vivo* topical administration of this probe is used to develop a standardized method to differentiate cancer from normal skin in excised human skin cancer specimens.

METHODS

Collection of human skin specimens

This study was approved by the University Hospitals Case Medical Center's IRB (IRB-protocol #12-05-17). Discarded skin tissues containing previously diagnosed BCC or SCC were taken during debulking for MMS (eTable) for this prospective case series. All BCC/SCC debulk specimens ≥ 1×1-cm were processed, imaged, and analyzed.

Ex vivo imaging of human skin specimens

Freshly removed debulk specimens were covered with saline-soaked gauze and delivered to the laboratory 90–120-min after surgery. Samples were rinsed with saline, blotted dry with gauze followed by baseline imaging (0-min). Probe GB119 (10 uM in DMSO; Sigma) was applied to the dermal side. After 5-min, excess probe was rinsed from the sample with saline and the dried sample was imaged in the Maestro Imaging System (Perkin Elmer) with a near-infrared filter set. Two sectioning approaches were used (eFigure 1/Graphical Abstract, step 4). In the bread-loaf section ink was used to mark the location of fluorescence before signals sectioning.

Analysis of Cy5-fluorescence

Fluorescence was measured and pseudo-color images were derived using a Maestro™ and supplied software 3.0.1.2 (Perkin Elmer). Levels of auto-fluorescence (0-min) were subtracted from fluorescence at 5-min with GB119 and remaining signal intensity was pseudo-colored. Signal was mapped onto the surface of the samples and inked in some cases. Samples were immersed in OCT compound, snap-frozen, and kept at −80°C for further study.

Histological and immunofluorescent analysis of human skin samples

Frozen blocks were sectioned (10-μm) in a bread-loaf manner at −30°C (Leica-CM3050S). The cryo-sections were then fixed and stained with H&E. For *en face* sectioning specimens were not inked and the entire frozen blocks were sectioned from dermal side toward epidermal side. Immunohistochemistry (IHC) for activated GB119 and cathepsin expression was performed on adjacent 10-μm sections for detection of unquenched/activated GB119 and cathepsin–L or –B, as described in Walker et al.[11]. Tissue nuclei were contrasted with Fluoro-Gel-II with DAPI (EMS).

Microscopy

Fluorescent images were viewed with a Leica-DM4000B microscope (bandpass=480/527, anti-cathepsin-L and -B and bandpass=560/645, anti-Cy5) and analyzed with QCapturePro-7 software. An Olympus-VS120/S5 versatile microscope-based scanner was used to generate histological images larger than a single field of view. Overlays between H&E and Cy5-fluorescent images were done manually. Technically validated results were included in the analyses and no data was excluded as "outliers". H&E examination of BCC/SCC slides was performed by two pathologists without knowledge of Cy5-fluorescent imaging or other

information. All annotations of the position of BCC/SCC as well as normal tissue were made by pathologists directly on the histological slides via marking pens.

Sensitivity and specificity analysis

Sensitivity and specificity were estimated as binomial proportions and exact 95% confidence intervals were calculated. The data set consisted of 55 samples from 54 patients (35 BCC and 20 SCC). A total of 72 histology sections (slides), containing 137 Regions of Interest (ROI) were examined. Ninety ROIs having tumor and 47 marked as having no tumor were treated as independent observations in a per-spot analysis; these sample sizes allowed estimation of overall sensitivity and specificity within ± 0.06 and 0.09 respectively using 95% confidence intervals when true sensitivity or specificity equal 0.90. The subtypes of all available samples are reported in the supplemental table.

RESULTS

QABP fluorescence discriminates between NMSC and normal tissue *ex vivo*

First we determined that normal human skin does not activate our imaging probe, GB119, after topical application (Figure 1A). Following topical application of GB119 to the non-epidermal surface of a sample containing either BCC or SCC there was significant probe activation resulting in increased fluorescence viewed *en face* (Figure 1B and C). Pathological correlation of the location of cancer and fluorescent signal in conventional bread-loaf sections taken from these specimens showed a good association and clear demarcation between normal and cancerous tissues (lower panels Figure 1B and C).

The sensitivity and specificity of the probe for detecting NMSC in BCC samples were 100% and 87%, respectively, Table 1. Similarly, using SCC samples only, the sensitivity and specificity were 97% and 92%, respectively, Table 1. There were no significant differences in probe activation among the subtypes of BCC and SCC and signal strength was significantly higher in NMSC versus normal skin, eTable and eFigure 7.

Presence of activated GB119 correlates with the expression of cathepsin-L in and around skin cancer

To further validate and characterize the relationship of probe activation with its cognate enzyme, IHC analysis was performed for cathepsin proteases (Figure 2). Bread-loaf sections were prepared from normal, BCC and SCC skin samples that were treated with GB119, and then underwent H&E staining and IHC for cathepsins and the activated probe. The results confirm that normal tissue expresses low levels of cathepsins and also shows little to no activation of the probe. Within cancer lesions, cathepsin expression was elevated and correlated to probe activation, with the highest probe signal and expression of cathepsins occurring at the edge of the cancer nests both in BCC and SCC (Figure 2). Controls confirmed the specificity of the assay (eFigure 2 in the Supplement). These studies also demonstrated that probe activation occurred in the thickest sample analyzed, approximately 2.5 mm (eTable and eFigure 8).

Fluorescence imaging defines the cancer diameter at different depths within the skin cancer lesion

Next 2D epi-fluorescence imaging of flat skin samples was correlated to the location of cancer within different depths of the skin specimens. Figure 3 shows a BCC skin sample that was topically treated with GB119, imaged (Figure 3A), frozen, and then *en face* sectioned followed by histology and IHC to identify the location of activated probe and NMSC. Sections from four different depths from the dermal site of application were assessed by blinded pathologists (Figure 3B, up to 0.8-mm and eFigure 8, up to 2.5 mm) and bolded contour lines representing the cancer (black/purple) and inflammation (red) perimeters at each depth were superimposed on the 2D-fluorescence image of the corresponding skin sample (Figure 3C), the larger distances representing the farthest distance from the dermal site of probe application.

These data show the heterogeneous location of the edge of cancerous tissue at different depths within the tissue specimens. The inflammatory milieu of cancer was found both inside and at the edge of the cancer lesions at different depths. As is evident in both Figure 3B and 3C the combination of the histology contour maps depicting cancer and its inflammatory milieu completely outline the fluorescence maps, demonstrating that the fluorescence signal, which comes from different depths within the lesion, accurately marks the perimeter of the cancerous lesion for BCC samples and potentially could be used to inform the location of peripheral margins for conventionally resected skin cancer. Similar results were obtained for SCC skin samples where sections at the depths up to 1.9-mm were analyzed by pathologists (see eFigure 3 and eTable).

To determine the exact correlation of fluorescence signal within cancer borders, the data from Figure 3 were used to identify regions depicting normal tissue, regions of cancer only, and the interface between cancer and normal tissues (rectangles, Figure 4A). These regions were then further analyzed to achieve a more detailed correlation of the location of cancer, cathepsin-L, and activated GB119 probe. Figure 4B–D show that there was a high degree of correlation between the presence of fluorescence and the location of BCC lesions and normal skin. Similar results were obtained for SCC samples, and inflammation associated with the sample was also observed in the regions with the highest level of GB119 activation and have demonstrated Cathepsin B is also associated with probe activation, (eFigures 4 and 5). The effect of blood clots affecting signal was demonstrated in eFigure 6.

DISCUSSION

The results of this study suggest a potentially promising approach to the surgical resection of NMSC, showing that the QABP GB119 topically applied to tissue after excision, can discriminate between normal skin and either BCC or SCC tissues within minutes. Following the procedure outlined in eFigure 1 these studies used 55 skin cancer specimens to demonstrate 90% or higher overall sensitivity and specificity for detecting BCC/SCC cancer lesions in a background of normal human tissue (Table and Figure 1). Further, subtypes of BCC (nodular, micronodular, superficial, and infiltrative) and SCC (well differentiated) were detected equally well by this technology, eTable and eFigure 7. Using an IHC assay for detection of activated GB119[11], it was possible to ascertain microscopic resolution of the

location of activated probe, protease expression, and cancerous cells showing that they co-localized at almost all locations, Figures 2 and 4. Comparing probe activation and pathological findings using *en face* sections at different depths below the application surface revealed that the perimeter of the 2D-fluorescence image reproducibly outlined the location of cancer at all depths assessed. Taken together, these data demonstrate that GB119/cathepsin-dependent fluorescent images of NMSC excisions discriminates cancerous tissue from normal skin defining the peripheral margins of BCC/SCC lesions and are not significantly affected by light scatter or diffusion by the tissue.

While previous efforts to enhance the detection and removal of skin cancer have resulted in the development of several optical fluorescence techniques[23–25], these approaches rely both on systemic and local administration of the imaging agents or imaging using endogenous differences in contrast. However, none of these methods have yet been clinically approved in the USA. For example, skin cancers investigators have attempted to utilize autofluorescence of skin cancer lesions[26], photodynamic diagnosis[27,28], or the use of a near-infrared fluorescent-labeled skin cancer targeted antibody, Panitumumab-IRDye800[29]. Each of these approaches, however, has drawbacks, resulting in lower sensitivity and specificity, longer times (6-hrs) for lesion discrimination, or the need for systemic injection with the potential of immunogenic response. Further the systemically administered agents require costly Phase I-III clinical trial to move towards clinical use. This approach utilizing topical application of imaging probes to detect cancer associated enzymes[10,30] is the only example to show *ex vivo* topical application of imaging probes to excised samples can rapidly visualize tumor margins during surgical procedures. Our previous studies demonstrated the feasibility of this approach using a brain tumor model[10] and now we use this technology to demonstrate for the first time its potential to impact conventional skin cancer resections in humans. We are currently conducting an IRB-approved trial to examine the specificity and sensitivity of this approach in the setting of such conventional wide local excisions. Ultimately, we envision this technology to inform the surgeon of margin status within 15 minutes of a conventional excision. This may enable surgeons to use minimal margins (e.g. 3mm vs. up to 5mm margins used for non-morpheaform BCCs) while obtaining similar or possibly more favorable recurrence rates. Commercialization of such a product would need to be economically viable to enable community practitioners to adopt this technology. Finally, we envision that this technology could improve health care access for superior margin control for those ineligible for MMS due to a variety of reasons; but QABP would not provide significant improvement as an additional step in modern MMS workflows.

In agreement with previous studies,[10,11,25,31] the data show close correlation between probe activation and the presence of cancer and areas of inflammation, which contain macrophages, activate GB119 and are presumably an important source of activated cathepsins. Areas of strong accumulation of macrophages (eFigure 4B, region 4) at the cancer lesion/normal tissue interface stained with both anti-cathepsin-L and for activated probe. Also GB119 activation occurs in the extracellular milieu of cancer cells, a likely result of the fact that cathepsins can be secreted from the cells. Since cathepsin-B (eFigure 5) expression is also associated with GB119 activation, it seems likely that Cy5-fluorescence imaging depends not only on presence of cathepsin-L but rather represents GB119/multi-cathepsin-dependent fluorescence from the top to bottom of the skin samples. These studies

demonstrate that overexpression of cathepsin proteases is prevalent in both BCC and SCC lesions making cathepsins an excellent biomarker for skin cancer margin detection.

The study also addressed potential limitations to this approach. A particular concern is the effect of surgery, tissue thickness, and tissue structures on the ability to visualize probe fluorescence. The presence of activated probe was detected in SCC zones but not in the cancer cell-free zones at the depth ~1.9-mm (eFigure 3B and 4B) and correlated to the deepest cancer in the specimens that were collected, 2.5 mm (eFigure 8). These depths of detection are well suited to detect cancer in the peripheral margins of the cancer indicating low impact, if any, of scattering or absorption of near-infrared light for imaging quality. In this study, we observed no difference in detection signal for the 4 subtypes of BCC and 2 subtypes of SCC examined (eFigure7). It will be critical to determine if this pattern is observed for other subtypes of BCC and SCC and to ensure that benign fibrosis/scarring in the absence of cancerous cells in addition to benign growths, e.g. do trichoepitheliomas produce a QABP signal similar to tumor.

Bleeding that might occur during sample preparation could cause another potential limitation to the technique (eFigure 6). Depending on the location, clot attenuation may compromise the ability to assess surgical margins *ex vivo*. However, blood clots in these samples were likely due to the transport time to the research lab, 90–120 min. Further development of imaging protocols will involve the use of only fresh-excised specimens imaged within 10-min of resection using a portable imaging device making them virtually free from clots as well as addressing other practical limitations of the approach presented here.

Supplementary Material

Refer to Web version on PubMed Central for supplementary material.

Acknowledgments

Funding/Support: This study was supported by an R21 (5R21CA183160-02) and P30 AR039750 P&F award (Dr. Basilion) and a subcontract to Dr. Basilion from an SBIR (5R21CA183160-02) awarded to Dr. Straight of Akrotome Imaging Inc.

Role of the Funder/Sponsor: The funding sources had no role in the design and conduct of the study; collection, management, analysis, and interpretation of the data; preparation, review, or approval of the manuscript; and decision to submit the manuscript for publication.

Abbreviations used

QABP	quenched activity-based probe
BCC	basal cell carcinomas
H&E	hematoxylin and eosin
IHC	Immunohistochemistry
MMS	Mohs micrographic surgery

NMSC	non-melanoma skin cancer
OCT	optimal cutting temperature
RT	room temperature
SCC	squamous cell carcinomas
2D	two dimensional
3D	three dimensional

References

1. Connolly SM, Baker DR, Coldiron BM, Fazio MJ, Storrs PA, Vidimos AT, et al. AAD/ACMS/ASDSA/ASMS 2012 appropriate use criteria for Mohs micrographic surgery: a report of the American Academy of Dermatology, American College of Mohs Surgery, American Society for Dermatologic Surgery Association, and the American Society for Mohs Surgery. J Am Acad Dermatol. 2012; 67(4):531–550. [PubMed: 22959232]
2. Rogers HW, Weinstock MA, Harris AR, Hinckley MR, Feldman SR, Fleischer AB, et al. Incidence estimate of nonmelanoma skin cancer in the United States, 2006. Arch Dermatol. 2010; 146(3):283–287. [PubMed: 20231499]
3. Rubin AI, Chen EH, Ratner D. Basal-cell carcinoma. N Engl J Med. 2005; 353(21):2262–2269. [PubMed: 16306523]
4. Mohs FE. Chemosurgical treatment of cancer of the skin; a microscopically controlled method of excision. JAMA. 1948; 138(8):564–569.
5. Mikhail, GR., editor. Mohs micrographic surgery. Philadelphia: W.B. Saunders; 1991.
6. Rowe DE, Carroll RJ, Day CL Jr. Prognostic factors for local recurrence, metastasis, and survival rates in squamous cell carcinoma of the skin, ear, and lip. Implications for treatment modality selection. J Am Acad Dermatol. 1992; 26(6):976–990. [PubMed: 1607418]
7. Griffiths RW. Audit of histologically incompletely excised basal cell carcinomas: recommendations for management by re-excision. Br J Plast Surg. 1999; 52(1):24–28. [PubMed: 10343586]
8. Motley R, Kersey P, Lawrence C. Multiprofessional guidelines for the management of the patient with primary cutaneous squamous cell carcinoma. Br J Dermatol. 2002; 146(1):18–25. [PubMed: 11841362]
9. Thomas DJ, King AR, Peat BG. Excision margins for nonmelanotic skin cancer. Plast Reconstruct Surg. 2003; 112(1):57–63.
10. Cutter JL, Cohen NT, Wang J, Sloan AE, Cohen AR, Panneerselvam A, et al. Topical application of activity-based probes for visualization of brain tumor tissue. PloS One. 2012; 7(3):e33060. [PubMed: 22427947]
11. Walker E, Gopalakrishnan R, Bogyo M, Basilion JP. Microscopic detection of quenched activity-based optical imaging probes using an antibody detection system: localizing protease activity. Mol Imaging Biol. 2014; 16(5):608–618. [PubMed: 24705781]
12. Jedeszko C, Sloane BF. Cysteine cathepsins in human cancer. Biol Chem. 2004; 385(11):1017–1027. [PubMed: 15576321]
13. Fröhlich E, Möhrle M, Klessen C. Cathepsins in basal cell carcinomas: activity, immunoreactivity and mRNA staining of cathepsins B, D, H and L. Arch Dermatol Res. 2004; 295(10):411–21. [PubMed: 14767779]
14. Kawada A, Hara K, Kominami E, Hiruma M, Akiyama M, Ishibashi A, et al. Expression of cathepsin D and B in invasion and metastasis of squamous cell carcinoma. Br J Dermatol. 1997; 137(3):361–366. [PubMed: 9349330]
15. Kawada A, Hara K, Kominami E, Kobayashi T, Hiruma M, Ishibashi A. Cathepsin B and D expression in squamous cell carcinoma. Br J Dermatol. 1996; 135(6):905–910. [PubMed: 8977710]

16. Ishida M, Kojima F, Okabe H. Cathepsin K expression in basal cell carcinoma. J Eur Acad Dermatol Venereol. 2013; 27(1):e128–130. [PubMed: 22220587]
17. Baruch A, Jeffery DA, Bogyo M. Enzyme activity – it's all about image. Trends Cell Biol. 2004; 14(1):29–35. [PubMed: 14729178]
18. Blum G, Mullins SR, Keren K, Fonovic M, Jedeszko C, Rice MJ, et al. Dynamic imaging of protease activity with fluorescently quenched activity-based probes. Nat Chem Biol. 2005; 1(4): 203–209. [PubMed: 16408036]
19. Blum G, von Degenfeld G, Merchant MJ, Blau HM, Bogyo M. Noninvasive optical imaging of cysteine protease activity using fluorescently quenched activity-based probes. Nat Chem Biol. 2007; 3(10):668–677. [PubMed: 17828252]
20. Sexton KB, Witte MD, Blum G, Bogyo M. Design of cell-permeable, fluorescent activity-based probes for the lysosomal cysteine protease asparaginyl endopeptidase (AEP)/legumain. Bioorg Med Chem Lett. 2007; 17(3):649–653. [PubMed: 17189693]
21. Kato D, Boatright KM, Berger AB, Nazif T, Blum G, Ryan C, et al. Activity-based probes that target diverse cysteine protease families. Nat Chem Biol. 2005; 1(1):33–38. [PubMed: 16407991]
22. Yuan F, Verhelst SH, Blum G, Coussens LM, Bogyo M. A selective activity-based probe for the papain family cysteine protease dipeptidyl peptidase I/cathepsin C. J Am Chem Soc. 2006; 128(17):5616–5617. [PubMed: 16637611]
23. de Boer E, Moore LS, Warram JM, Huang CC, Brandwein-Gensler MS, van Dam GM, et al. On the horizon: Optical imaging for cutaneous squamous cell carcinoma. Head Neck. 2015 Apr 20.doi: 10.1002/hed.24079
24. Mitsunaga M, Kosaka N, Choyke PL, Young MR, Dextras CR, Saud SM, et al. Fluorescence endoscopic detection of murine colitis-associated colon cancer by topically applied enzymatically rapid-activatable probe. Gut. 2013; 62(8):1179–1186. [PubMed: 22698650]
25. Verdoes M, Edgington LE, Scheeren FA, Leyva M, Blum G, Weiskopf K, et al. A nonpeptidic cathepsin S activity-based probe for noninvasive optical imaging of tumor-associated macrophages. Chem Biol. 2012; 19(5):619–628. [PubMed: 22633413]
26. Brancaleon L, Durkin AJ, Tu JH, Menaker G, Fallon JD, Kollias N. In vivo fluorescence spectroscopy of nonmelanoma skin cancer. Photochem Photobiol. 2001; 73(2):178–183. [PubMed: 11272732]
27. Kamrava SK, Behtaj M, Ghavami Y, Shahabi S, Jalessi M, Afshar EE, et al. Evaluation of diagnostic values of photodynamic diagnosis in identifying the dermal and mucosal squamous cell carcinoma. Photodiagnosis Photodyn Ther. 2012; 9(4):293–298. [PubMed: 23200008]
28. Jeon SY, Kim KH, Song KH. Efficacy of photodynamic diagnosis-guided Mohs micrographic surgery in primary squamous cell carcinoma. Dermatol Surg. 2013; 39(12):1774–1783. [PubMed: 24299572]
29. Heath CH, Deep NL, Beck LN, Day KE, Sweeny L, Zinn KR, et al. Use of panitumumab-IRDye800 to image cutaneous head and neck cancer in mice. Otolaryngol Head Neck Surg. 2013; 148(6):982–990. [PubMed: 23525846]
30. Urano Y, Sakabe M, Kosaka N, Ogawa M, Mitsunaga M, et al. Rapid Cancer Detection by Topically Spraying a γ-Glutamyltranspeptidase–Activated Fluorescent Probe. Science Translational Medicine. Nov 23.2011 3(110):110ra119.
31. Segal E, Prestwood TR, van der Linden WA, Carmi Y, Bhattacharya N, Withana N, et al. Detection of intestinal cancer by local, topical application of a quenched fluorescence probe for cysteine cathepsins. Chem Biol. 2015; 22(1):148–158. [PubMed: 25579207]

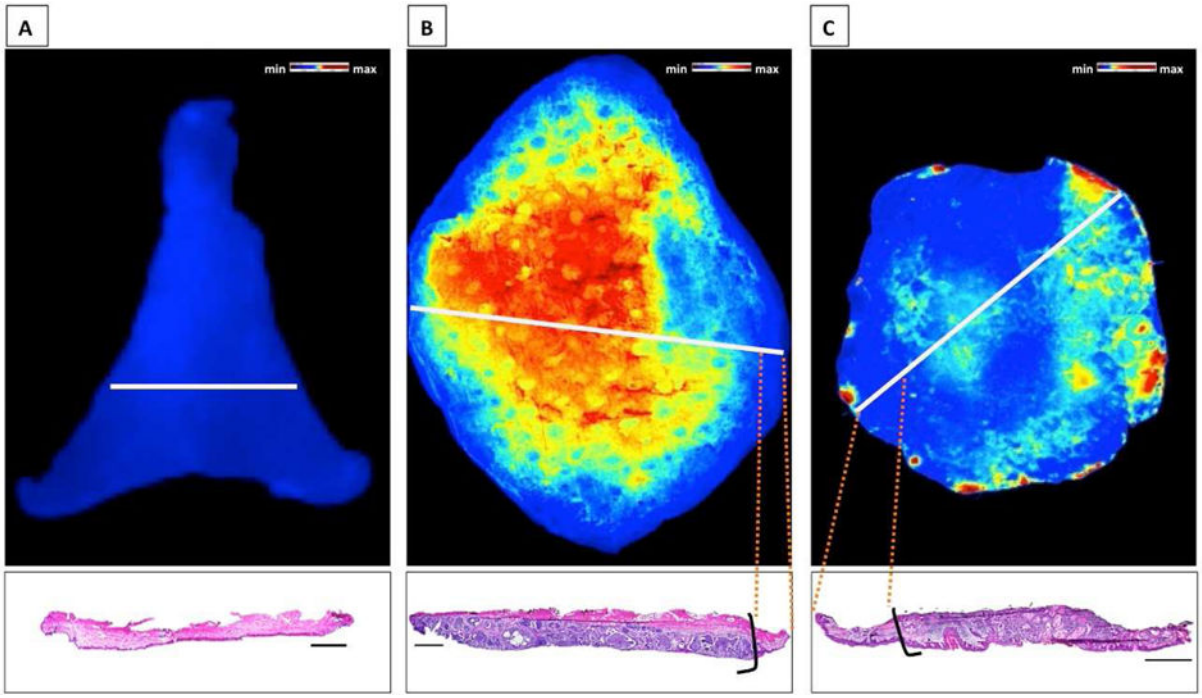

Figure 1. Bread-loafed Skin Cancers: Probe activation corresponds to the presence of cancer

Activation of GB119 and corresponding pathology from bread-loaf sections of specimens. **A**, Normal tissue. **B**, BCC. **C**, SCC. Presence of pathology ink on the dermal side of the samples that was used to mark the areas of high Cy5-fluorescence. *White lines* – plane of section. *Black lines* demark the cancer zone borders. *Scale Bars* = 2 mm.

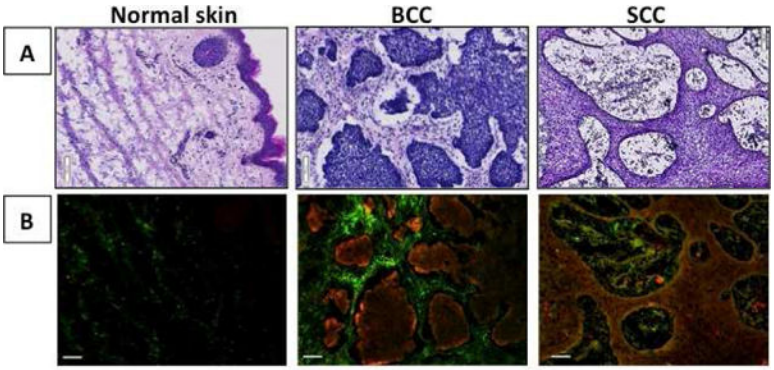

Figure 2. Basal Cell and Squamous Cell Carcinomas: Correlation of probe activation to cancer and cathepsin-L expression in BCC/SCC samples

A, H&E histology of bread-loaf sections of human skin samples pretreated with GB119. **B**, IHC of the bread-loaf section shows co-localization of cathepsin-L (green) and Cy5 (activated probe, red) in image overlays. Scale bars = 100 μm.

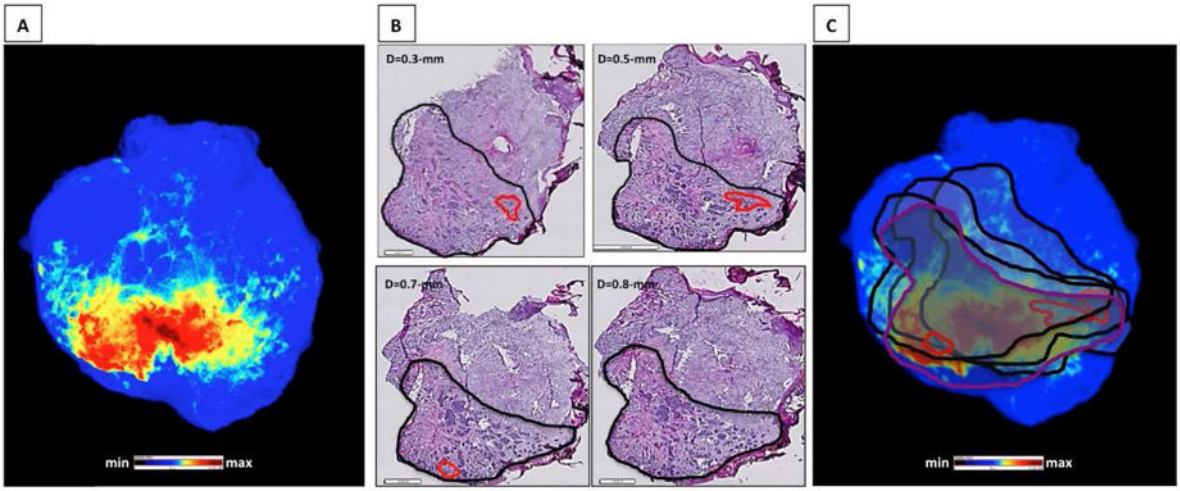

Figure 3. Basal Cell Carcinoma: Correlation of pathology throughout the BCC specimen with epi-fluorescence imaging

A, Cy5-fluorescent image of skin sample pre-treated with GB119. **B**, *En face* section histology at different depth; *bold contour markings* = pathologist H&E mapped cancer perimeter. **C**, Overlay of contour markings on the fluorescence image of the skin sample; *red contours* = tissue inflammation. Scale bars (H/E) – 1-mm and 2-mm (large).

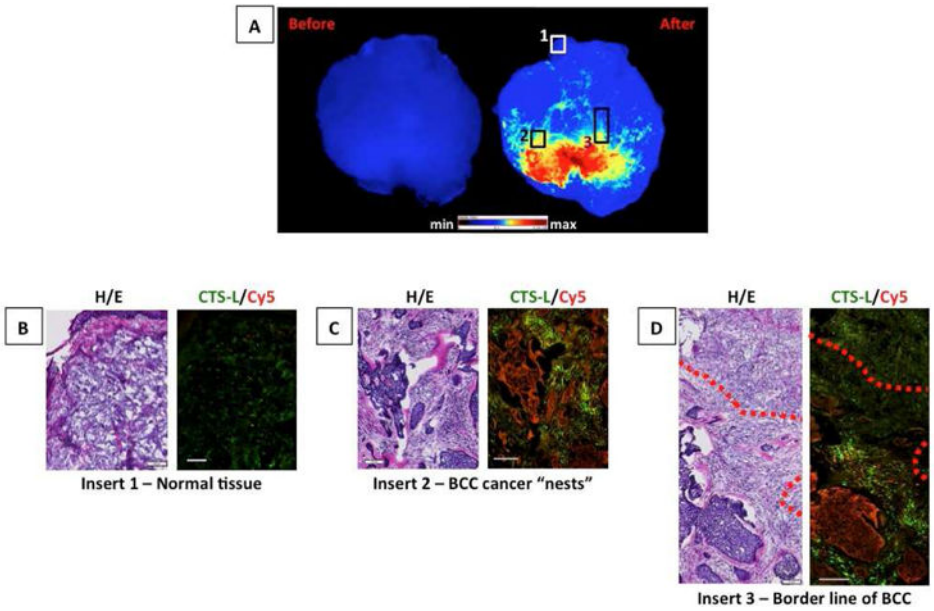

Figure 4. Basal Cell Carcinoma: Microscopic analysis of regions representing different locations within the sections

A, Fluorescent images of BCC skin specimen treated with GB119. **B** – **D**, Overlay of cathepsin-L (green) and Cy5 (red) from different locations of the sample; *red dotted line* = borderline between BCC and normal tissue. *Scale bars* = 100 μm.

Table

Analysis of relationship between GB119 activation and presence of skin cancer in human skin samples

Measure	Group Examined	Regions of Interest (ROIs)	Sensitivity/Specificity	95% Confidence Interval (2-sided)
Sensitivity	All patients	90	0.989 (89/90)	0.940–1.000
	BCC only	56	1.000 (56/56)	0.936–1.000
	SCC only	34	0.971 (33/34)	0.847–1.000
Specificity	All patients	47	0.894 (42/47)	0.769–0.965
	BCC only	23	0.870 (20/23)	0.664–0.972
	SCC only	24	0.917 (22/24)	0.730–0.990

For these studies 55 patient samples were assessed. These samples included 35 BCC (N=8, MN=10, I=4, and S=8, M=5) and 20 SCC (WD=15, MD=3, PD=0, M=2) specimens. **BCC** – basal cell carcinoma; N – nodular, MN – micro-nodular, S – superficial, and I – infiltrative form of BCC; **SCC** – squamous cell carcinoma; WD – well differentiated, MD – mildly differentiated, and PD – poorly differentiated of SCC. M=mixed pathology for either BCC or SCC.